Heat conduction in graphene flakes with inhomogeneous mass interface

J. Stat. Mech. (2011) P10031

(http://iopscience.iop.org/1742-5468/2011/10/P10031)

Journal of Statistical Mechanics: Theory and Experiment
An IOP and SISSA journal

Heat conduction in graphene flakes with inhomogeneous mass interface

Jigger Cheh[1] **and Hong Zhao**[1,2]

[1] Department of Physics, Institute of Theoretical Physics and Astrophysics, Xiamen University, Xiamen 361005, People's Republic of China
[2] State Key Laboratory for Nonlinear Mechanics, Institute of Mechanics, Chinese Academy of Sciences, Beijing 100080, People's Republic of China
E-mail: jk_jigger@xmu.edu.cn and zhaoh@xmu.edu.cn

Received 7 August 2011
Accepted 7 October 2011
Published 31 October 2011

Online at stacks.iop.org/JSTAT/2011/P10031
doi:10.1088/1742-5468/2011/10/P10031

Abstract. Using nonequilibrium molecular dynamics simulations, we study the heat conduction in graphene flakes composed by two regions. One region is mass-loaded and the other one is intact. It is found that the mass interface between the two regions greatly decreases the thermal conductivity, but it would not bring about a thermal rectification effect. The dependence of thermal conductivity upon the heat flux and the mass difference ratio is studied to confirm the generality of the result. The interfacial scattering of solitons is studied to explain the absence of the rectification effect.

Keywords: transport processes/heat transfer (theory), heat conduction

J. Stat. Mech. (2011) P10031

1742-5468/11/P10031+11$33.00

Thermal rectification is a phenomenon when the heat flux runs preferentially along one direction and inferiorly along the opposite direction [1]–[14]. It has attracted a great deal of attention in the last decade since it reveals the possibility to control the heat transportation process. With an improved understanding of thermal rectification, various devices like thermal transistors, thermal logic circuits and thermal diodes could be fabricated. Two methods are commonly used to design thermal rectifiers. The first method is to couple two or more anharmonic chains with different nonlinear potentials together [3]–[5]. The explanation for the observed rectification effect is that the phonon bands of different regions of the chain will change from overlap to separation when the heat flux is reversed. The asymmetry of the interaction potential controls the phonon band shift and it plays the central role here. The second method is to implement asymmetric geometric shapes in quasi-1D and 2D systems. For example, it is applied in deformed carbon nanotubes [6], carbon nanohorns [7], and triangular-shaped, trapezoid-shaped and U-shaped graphene flakes [8]–[10]. Thermal conductivity is higher when the heat flux runs from the narrow to the wide region. The explanation for the observed rectification is that the asymmetric geometric shape introduces asymmetric boundary scattering of phonons. The asymmetry of the geometric shape controls the phonon scattering and it plays a central role in this case.

Recently a new procedure is considered by Chang *et al* in carbon and boron nitride nanotubes [11]. They introduce the asymmetry of mass distribution by covering an external platinum compound on the nanotubes. Comparing with nanotubes, the thermal contribution of the platinum compound can be neglected. So the mass-loading procedure is idealized by Chang *et al* as changing the atomic mass of the atoms in the heat conduction process. Higher thermal conductivity is observed when the heat flux runs from the heavy mass region to the light mass region. However, the observed rectification effect cannot be explained by phonons. First, the externally loaded molecules do not contribute to any bond, thus the anharmonic coupling between the atoms in the nanotubes is not changed. The asymmetry of the interaction potential does not contribute here. Second, the associated geometric deformation of the nanotubes is not dominant, thus the boundary scattering of phonons is also not changed. The asymmetry of the geometric shape also does not contribute in this case. Then Chang *et al* surmise that the origin of the rectification effect is due to the asymmetric interfacial scattering between the two regions with inhomogeneous mass. However, as pointed out by Change *et al*, it is well known that the interfacial scattering of phonons is independent of the incident direction. Therefore they postulate that solitons are responsible for the asymmetric interfacial scattering process. Later a similar thermal rectification effect has been observed in molecular dynamic simulations of mass-graded carbon nanotubes [12]–[14]. In the simulations, the atomic mass of carbon atoms is gradually increased from 12 to 300 along the axis of the tubes. The set-up is treated as a combination of multiple inhomogeneous mass interfaces.

Graphene [15, 16], a single layer of carbon atoms in a honeycomb lattice with sp^2 bonds, reveals superior high thermal conductivity up to 2500–5000 W m K^{-1} at room temperature [17, 18]. It has been considered as a promising candidate for various thermal devices. Graphene is similar to carbon nanotubes in both structure and thermal properties, so it is interesting to know whether thermal rectification would occur if the

J. Stat. Mech. (2011) P10031

mass interface is implemented. Besides, managing heat transportation across the interface is very common in nanoelectronic design. Thus it is also interesting to understand the influence of the mass interface upon the thermal conductivity of graphene.

Here we study the heat conduction in graphene flakes with an inhomogeneous mass interface between two regions by NEMD (nonequilibrium molecular dynamics) simulations. The graphene flakes are composed by two regions. One region is intact and the other region is externally mass-loaded. For simplicity, the mass-loaded region is realized by modulating the atomic mass of carbon atoms in the molecular dynamics simulations. This set-up is widely accepted as the idealized method for the mass-loading procedure [12]–[14]. We report that the thermal rectification effect does not exist even if a large mass difference ratio is implemented. In order to understand the microscopic mechanism leading to the absence of the thermal rectification effect, we also study the interfacial scattering of solitons in graphene.

We carry out the molecular dynamics simulations of the heat conduction in two rectangular graphene flakes with zigzag edges along the x axis and armchair edges along the y axis. The graphene flakes are shown in figure 1(a). They are both 288 Å long and 21 Å wide. The heat sources and heat sinks are covered by red boxes with 100 carbon atoms. The outmost edges of the heat sources/sinks are frozen. It corresponds to fixed boundary conditions in the y axis. A periodic boundary condition is used along the x axis. The atomic mass of the intact carbon atoms is $m_0 = 12$ and they are drawn in cyan. The atomic mass of the mass-loaded carbon atoms is $m_N \geqslant 12$ and they are drawn in silver. The upper half region of the first graphene flake in figure 1(a) is mass-loaded, thus we label it as the m_0–m_N graphene flake. Similarly we label the second one in figure 1(a) as the m_N–m_0 graphene flake. The heat flux running along the m_N–m_0 graphene flake is equivalent to the reversed heat flux running along the m_0–m_N graphene flake. The thermal conduction process is investigated by imposing the same heat flux along the two graphene flakes. It is much more convenient later to compare the temperature profiles since the heat sources and heat sinks are in the same direction. We use the same reactive empirical bond-order (REBO) potential [19] as implemented in the LAMMPS [20] code to simulate the anharmonic coupling between the carbon atoms. Equations of motions are integrated with the velocity Verlet algorithm with the minimum timestep $\Delta t = 0.25$ fs.

First the graphene flakes are equilibrated at a constant temperature $T = 300$ K in the Nose–Hoover thermostat by 0.75 ns. After that the heat flux is imposed. It is realized by the energy and momentum conserving velocity rescaling algorithm developed by Jude and Jullien [21]. A constant rate of kinetic energy $\mathrm{d}E$ is added in the heat source and removed in the heat sink at each time step $\mathrm{d}t$. The heat flux is calculated as $J = \mathrm{d}E/\mathrm{d}t$. It is widely used to study the interfacial heat conduction in different materials [22]–[24]. We divide the graphene flakes by several 4 Å long slabs along the y axis to obtain the temperature profiles. Each slab contains about 60–70 carbon atoms. The local temperature in each slab is calculated from the averaged kinetic energy of the carbon atoms. The temperature profiles are averaged over every 100 ps after the heat flux is imposed. The whole nonequilibrium simulation process covers 3 ns and the last 1 ns is utilized as the steady state since the temperature profiles do not change much. Thermal conductivity G of the whole graphene flake is calculated by Fourier's law:

$$G = -\frac{J/A}{\Delta T/\Delta L}. \tag{1}$$

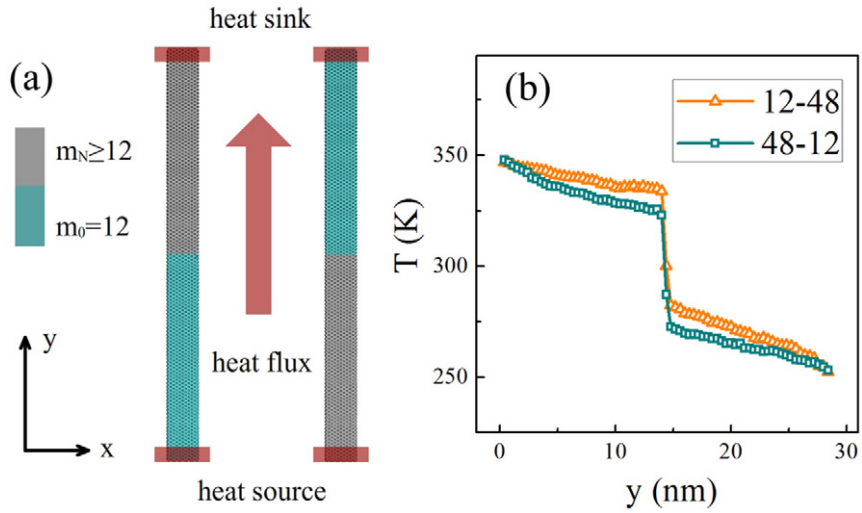

Figure 1. (a) Schematic of the graphene flakes with inhomogeneous mass interface. The first one is labeled as the m_0–m_N graphene flake. The upper region of the m_0–m_N graphene flake is mass-loaded, which is simplified by modulating the atomic mass of the carbon atoms as $m_N \geqslant 12$. Similarly the second one is labeled as the m_N–m_0 graphene flake. The lower region of the m_N–m_0 graphene flake is mass-loaded. (b) The typical temperature profiles of the two graphene flakes in the heat conduction process. Here $m_N/m_0 = 4$ and $J = 0.35$ eV ps^{-1} are implemented. The 12–48 and 48–12 graphene flakes exhibit the same temperature drop near the mass interface and between the two ends along the whole simulation cell.

Here J is the heat flux and A is the cross section of the heat transfer defined by the product of the width and the thickness of the graphene flakes. The thickness of the graphene flake is usually considered as the bond length of the carbon atoms and it is taken as 1.4 Å in our computation [25, 26]. ΔT (ΔL) is the temperature (distance) difference between the two ends on the graphene flake. Thermal conductivity G represents the thermal conducting capacity of the whole graphene flake. eV ps^{-1} is selected as the unit for the heat flux, Å is selected as the unit for the width and thickness, K is selected as the unit for the temperature. W m K^{-1} is selected as the unit for the thermal conductivity, so the associated numerical results are converted to this unit.

In figure 1(b) we show the typical temperature profiles of the two graphene flakes. Here $m_N/m_0 = 4$ and $J = 0.35$ eV ps^{-1} are implemented. A sudden temperature drop is observed near the mass interface. It indicates that the mass interface behaves like a strong thermally resistive boundary. In figure 1(b), it also shows that, although the temperature profiles are different in the two graphene flakes, the temperature differences between the two ends are the same. The temperature difference in the 12–48 graphene flake is 94.0 K and the temperature difference in the 48–12 graphene flake is 93.8 K. Thus the thermal conductivity G of the two graphene flakes is the same. It indicates that, even for such a large temperature difference, there is still no observable thermal rectification effect. The 12–48 and the 48–12 graphene flakes have the same thermal conducting capacity and the heat flux runs equivalently without a preferred direction.

J. Stat. Mech. (2011) P10031

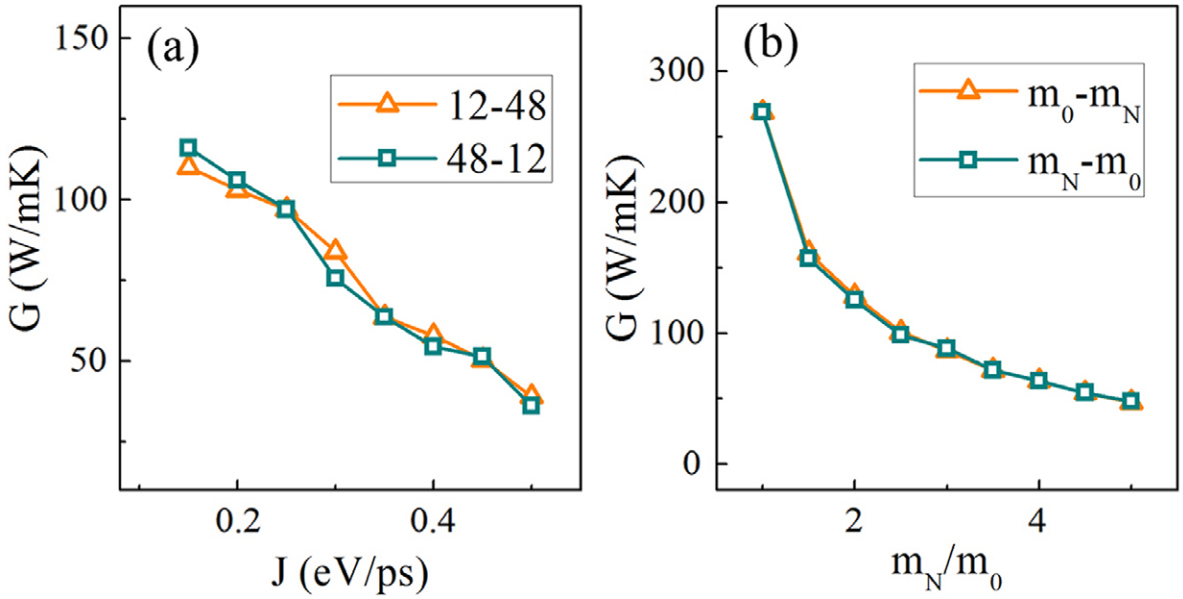

Figure 2. (a) Thermal conductivity G versus heat flux J. Here the mass difference ratio $m_N/m_0 = 4$ is unchanged and the heat flux J varies from 0.15 to 0.5 eV ps^{-1}. (b) Thermal conductivity G versus the mass difference ratio m_N/m_0. Here the heat flux $J = 0.35$ eV ps^{-1} is unchanged and the mass difference ratio varies from 1 to 5. For $m_N/m_0 = 1$, the thermal conductivity G is obtained from the graphene flake without the mass interface.

In order to further confirm the result that there is no thermal rectification effect brought about by the mass interface in the graphene flakes, the dependence of thermal conductivity upon the heat flux and the mass difference ratio is studied. First we keep the mass difference ratio $m_N/m_0 = 4$ invariant and vary the heat flux from 0.15 to 0.5 eV ps^{-1}. In figure 2(a) we show the dependence of thermal conductivity upon the heat flux. Thermal conductivity is almost the same in the two graphene flakes. It indicates that there is no thermal rectification effect by using a different value of heat flux. Meanwhile it is found that thermal conductivity is decreasing with the heat flux. For $J = 0.15$ eV ps^{-1}, the thermal conductivity is about 110 W m K^{-1}. For $J = 0.5$ eV ps^{-1}, it is reduced to 38 W m K^{-1} which is about 35% of the original value. It indicates that interfacial scattering is enhanced by the amount of heat flux and the effect might be taken into consideration in real application.

Second, we keep the heat flux $J = 0.35$ eV ps^{-1} invariant and vary the mass difference ratio m_N/m_0 from 1 to 5. Here $m_N/m_0 = 1$ stands for the graphene flake without the mass interface. In figure 2(b) we show the dependence of thermal conductivity upon the mass difference ratio. Thermal conductivity is almost the same in the two graphene flakes. It indicates there is no thermal rectification effect by using a different mass difference ratio. Meanwhile it is found that thermal conductivity is greatly decreased by the mass interface. The thermal conductivity of the graphene flake without the mass interface is about 269 W m K^{-1}. When the mass interface is implemented ($m_N/m_0 = 5$), it is reduced to 45 W m K^{-1}. It is only about 16% of the original value. Here it provides

doi:10.1088/1742-5468/2011/10/P10031

J. Stat. Mech. (2011) P10031

a possible route to tune the thermal behavior of graphene. The mass interface can be implemented by two methods. One is to load external heavy and thermally insulating molecules upon the carbon atoms [11]–[14]. The other one is to use different ratios of isotope substitutions [27]–[29] which is demonstrated as possible in experiments by chemical vapor deposition growth of graphene on metal [30].

The heat conduction results suggest that inhomogeneous mass interface cannot lead to the thermal rectification effect in graphene. In the above simulations, the anharmonic coupling between the carbon atoms is kept constant and there is no geometric deformation by using periodic boundary condition along the width. Therefore, just like carbon nanotubes, the asymmetry of the interaction potential and the asymmetry of the geometric shape also do not contribute in the graphene flakes. Furthermore, the interfacial scattering of solitons in surmised to be responsible for the thermal rectification effect in carbon nanotubes [11]. So in order to understand the absence of the thermal rectification effect, it is necessary to study the interfacial scattering of solitons in graphene. Recently, subsonic NLS (nonlinear Schrödinger) equation-described solitons are found in graphene [31]. They preserve their identities in propagation and exhibit strong interactions and phase shifts in collisions. Their energy reflection rates between the two regions with different masses are needed if one tends to know whether the solitons would bring a rectification effect in the interfacial scattering process [32]–[34].

Here we first generate a longitudinal soliton in a 485 nm long graphene flake with atomic mass $m_0 = 12$. The chirality of the graphene flake is the same as the two graphene flakes in figure 1(a). In the curve t_1 of figure 3(a), we show the longitudinal velocity (vy) distribution of the carbon atoms before the interfacial scattering. The soliton is set as the incident soliton and its amplitude is positive. After that we change the atomic mass of the carbon atoms ahead of the solitons to be $m_N = 48$ to set up a mass interface. The barrier line in the middle of figure 3(a) separates the graphene flake into two regions. The atomic mass of the left region is intact ($m_0 = 12$) and the atomic mass of the right region is mass-loaded ($m_N = 48$). The interfacial scattering from the m_0 to the m_N region happens when the incident soliton hits the mass interface. In the curve t_2 of figure 3(a), we show the longitudinal velocity distribution of the carbon atoms after the interfacial scattering. The incident soliton is scattered to a transmitted soliton and a reflected soliton. The amplitude of the transmitted soliton is positive and the amplitude of the reflected soliton is negative in the 12–48 scattering. Similarly we obtain the interfacial scattering from the m_N to the m_0 region. In figure 3(b) we show that the amplitude of the transmitted soliton is positive and the amplitude of the reflected soliton is also positive in the 48–12 scattering. The scattering results indicate that the amplitude of the reflected soliton is dependent upon the incident direction. It is negative in the m_0–m_N scattering and positive in the m_N–m_0 scattering. Such behavior of the reflected soliton has also been obtained in the interfacial scattering of similar NLS solitons in 1D nonlinear chains [32]. It represents a different kinetic behavior of the NLS solitons from the KdV solitons which have no reflected solitons in the m_N–m_0 scattering.

There is a rescaling relation between the width of the scattered solitons. The propagating velocity of a soliton in the m_0 region is 20 km s^{-1} and in the m_N section [31] is $v(m_N) = [\cos(kl_0/2) - (\alpha + A\tan\varphi/2\sqrt{\sigma})\sin(kl_0/2)]\sqrt{b/m_N} \propto 1/\sqrt{m_N}$. Since the scattering time Δt is very short we can thus neglect the amplitude-dependent parameters in the formula to estimate Δt. In the m_0–m_N scattering Δt can be estimated by the

J. Stat. Mech. (2011) P10031

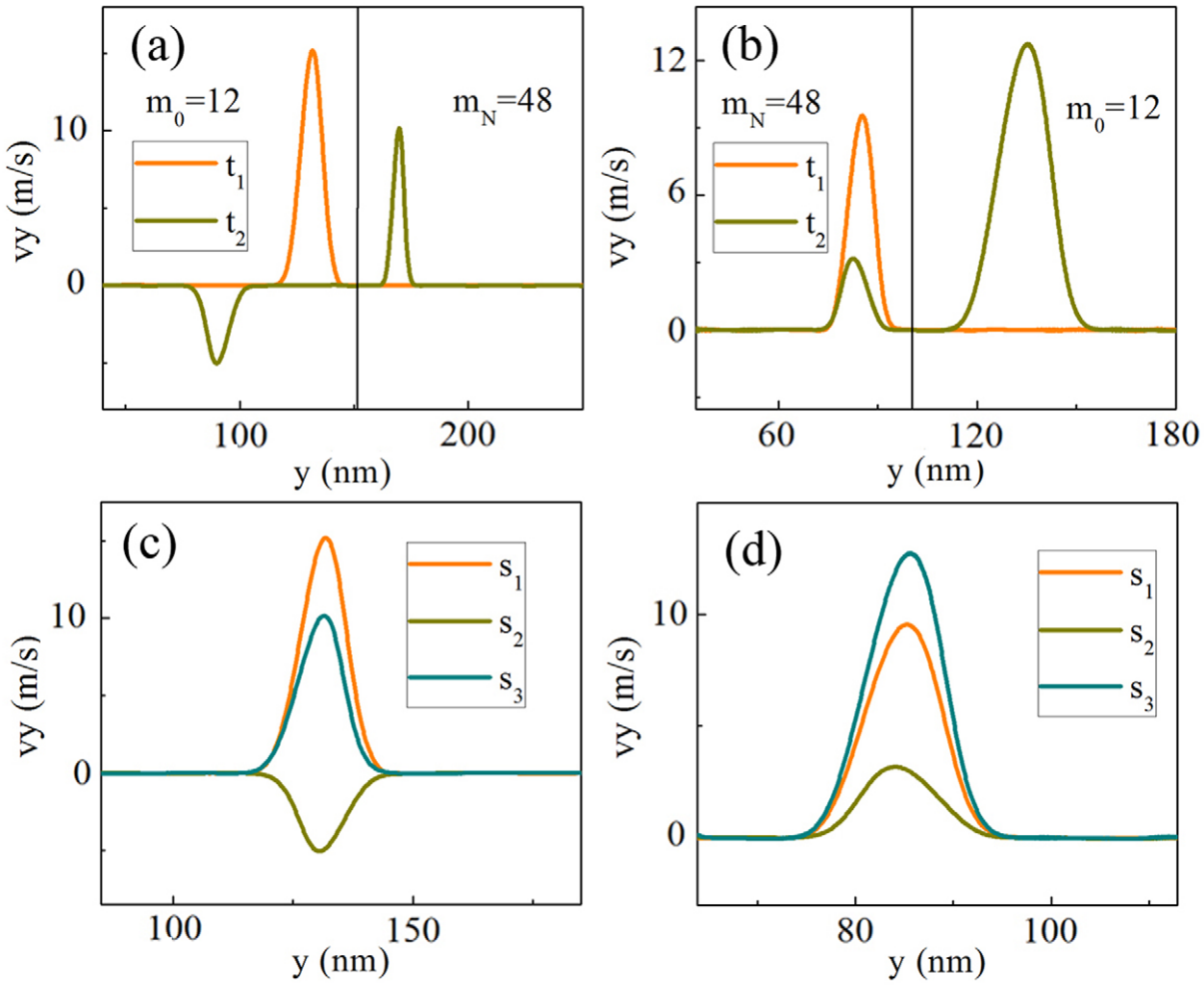

Figure 3. (a), (b) The barrier line in the middle of (a) and (b) separates the graphene flake into two regions. The atomic mass of the m_0 region is 12. The atomic mass of the m_N region is 48. The curve t_1 represents the longitudinal velocity of the carbon atoms before the scattering. The curve t_2 represents the longitudinal velocity of the carbon atoms after the scattering. The time interval between t_1 and t_2 is 3.2 ps. The 12–48 scattering is shown in (a). The 48–12 scattering is shown in (b). (c), (d) Rescaling the width of the reflected soliton s_2 and the transmitted soliton s_3 according to the width of the incident soliton s_1. The rescaling in the 12–48 scattering is shown in (c). The rescaling in the 48–12 scattering is shown in (d).

width of the incident soliton $w^{\mathrm{I}}_{m_0-m_N}$ as $\Delta t = w^{\mathrm{I}}_{m_0-m_N}/20$. So the width of the reflected soliton $w^{\mathrm{R}}_{m_0-m_N}$ in the m_0 region and the width of the transmitted soliton $w^{\mathrm{T}}_{m_0-m_N}$ in the m_N region are

$$w^{\mathrm{R}}_{m_0-m_N} = 20\Delta t = w^{\mathrm{I}}_{m_0-m_N} \tag{2}$$

$$w^{\mathrm{T}}_{m_0-m_N} = v(m_N)\Delta t = \frac{\sqrt{m_0}}{\sqrt{m_N}} w^{\mathrm{I}}_{m_0-m_N}. \tag{3}$$

Similar relations can be obtained in m_N–m_0 scattering. The width of the reflected soliton $w^{\mathrm{R}}_{m_N-m_0}$ in the m_N region and the width of the transmitted soliton $w^{\mathrm{T}}_{m_N-m_0}$ in the m_0 region are

$$w^{\mathrm{R}}_{m_N-m_0} = w^{\mathrm{I}}_{m_N-m_0} \tag{4}$$

$$w^{\mathrm{T}}_{m_N-m_0} = \frac{\sqrt{m_N}}{\sqrt{m_0}} w^{\mathrm{I}}_{m_N-m_0}. \tag{5}$$

In figures 3(c) and (d) we show the width rescaling relations between the scattered solitons. The width of the reflected soliton s_2 and the transmitted soliton s_3 are rescaled well according to the width of the incident soliton s_1.

In order to understand the role of solitons play in the heat conduction process, the energy reflection rate is needed. We measure the energy E and the momentum P of a soliton in graphene as the aggregated momentum and energy of all the carbon atoms along the width of the soliton [35, 36]:

$$E = \sum_k \tfrac{1}{2} m v_k^2 + E_k^{\mathrm{REBO}} \qquad P = \sum_k m v_k. \tag{6}$$

Here only the carbon atoms with $\|v_k\| > 0.01$ m s^{-1} are counted. The widths of the scattered solitons could also be estimated by the rescaling relation in equations (2)–(5). When the energy and the momentum of the scattered solitons are obtained, the energy reflection rate R^E and the momentum reflection rate R^P are defined as

$$R^E = \frac{E^{\mathrm{R}}}{E^{\mathrm{I}}} \times 100\% \qquad R^P = \frac{P^{\mathrm{R}}}{P^{\mathrm{I}}} \times 100\%. \tag{7}$$

Here E^{I} and P^{I} are the energy and the momentum of the incident soliton. E^{R} and P^{R} are the energy and the momentum of the reflected soliton.

In figure 4 we show the dependence of the energy and the momentum reflection rate upon the mass difference ratio. In figure 4(a) it shows that the energy reflection rates in the m_0–m_N and the m_N–m_0 scattering are the same. In figure 4(b) it shows that the momentum reflection rates are asymmetric. In the m_0–m_N (m_N–m_0) scattering, the negative (positive) momentum reflection rates are obtained. The results explain the absence of thermal rectification in graphene: although the momentum reflection rate is dependent upon the incident direction, the energy reflection rate is direction-independent. The same amount of energy would be reflected by the mass interface; thus it brings no reflection effect into the heat conduction process.

Here we point out that the role the KdV solitons surmised by Chang *et al* plays in thermal rectification is still under heavy debate [1], [12]–[14], [37]. First, an extremely large excitation is needed to generate the supersonic KdV solitons. In carbon nanotubes, they are surmised to be generated by the collision of electrons, ultrashort laser light or strong compressions [38, 39]. So it is almost impossible that, in the heat conduction process at room temperature, the KdV solitons could be generated. So far there is still no direct evidence of the supersonic KdV solitons in either carbon nanotubes or graphene flakes. Second, Chang *et al* suggest the preferred direction of the heat flux is from the heavy to the light mass regions by considering KdV solitons [11]. However, in the MD simulations of carbon nanotubes, it shows that the preferred direction is from the light to the heavy mass regions. It contradicts the existence of the KdV solitons in carbon

J. Stat. Mech. (2011) P10031

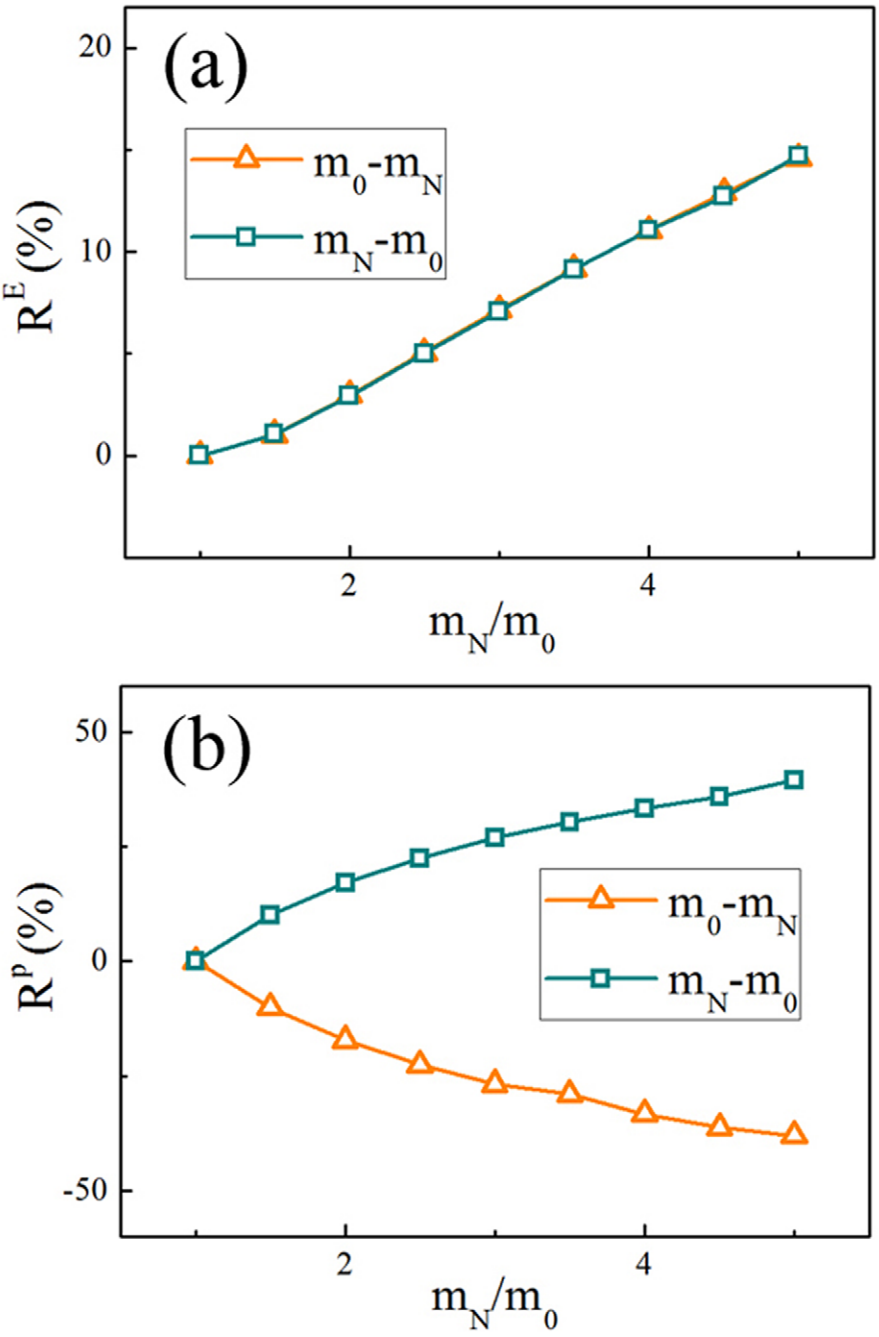

Figure 4. Here $m_0 = 12$ and m_N vary from 12 to 60. For $m_N/m_0 = 1$, it stands for the case that there is no mass interface in the graphene flake. Thus the energy and the momentum reflection rates are both 0 in this case. (a) Energy reflection rate R^E versus mass difference ratio m_N/m_0. (b) Momentum reflection rate R^P versus mass difference ratio m_N/m_0.

J. Stat. Mech. (2011) P10031

nanotubes [12]–[14]. In our molecular dynamics simulations of graphene flakes, there is no thermal rectification effect in the heat conduction process. The result is also against the existence of the KdV solitons in graphene. Third, the square of the amplitudes is used to estimate the energy of a soliton by Chang *et al*. However, the dependence of energy upon the amplitude is far more complicated [35, 36]. Thus the width of a soliton is also necessary to be taken into consideration in order to measure the amount of energy.

In summary, the inhomogeneous mass interface cannot introduce the thermal rectification effect in graphene. The absence of the rectification effect is confirmed by studying different heat flux and mass difference ratios. The microscopic mechanism is explained by the interfacial scattering of solitons in graphene which reveals a direction-independent energy reflection rate. Our results imply that the mass interface or the mass gradient which is a combination of multiple mass interfaces cannot be applied to design graphene-based thermal rectifiers.

Acknowledgments

We thank Jiao Wang and Yong Zhang for helpful discussion and preparation of the manuscript. This work was supported by the National Natural Science Foundation of China (nos. 10775115 and 10925525).

References

[1] Casati G, 2007 *Nature Nanotechnol.* **2** 23
[2] Roberts N A and Walker D G, 2011 *Int. J. Therm. Sci.* **50** 648
[3] Terraneo M, Peyrard M and Casati G, 2002 *Phys. Rev. Lett.* **88** 094302
[4] Li B, Wang L and Casati G, 2004 *Phys. Rev. Lett.* **93** 184301
[5] Hu B, Yang L and Zhang Y, 2006 *Phys. Rev. Lett.* **97** 124302
[6] Wu G and Li B, 2007 *Phys. Rev.* B **76** 085424
[7] Wu G and Li B, 2008 *J. Phys.: Condens. Matter* **20** 175211
[8] Hu J, Ruan X and Chen Y P, 2009 *Nano Lett.* **9** 2730
[9] Yang N, Zhang G and Li B, 2009 *Appl. Phys. Lett.* **95** 211908
[10] Cheh J and Zhao H, 2011 arXiv:1108.5270v1 [cond-mat.mtri-sci]
[11] Chang C W, Okawa D, Majumdar A and Zettl A, 2006 *Science* **314** 1121
[12] Alaghemandi M, Algaer E, Bohm M C and Müller-Plath F, 2009 *Nanotechnology* **20** 115704
[13] Alaghemandi M, Leroy F, Algaer E, Bohm M C and Müller-Plath F, 2010 *Nanotechnology* **21** 075704
[14] Alaghemandi M, Leroy F, Algaer E, Müller-Plath F and Bohm M C, 2010 *Phys. Rev.* B **81** 125410
[15] Geim A K and Novoselov K S, 2007 *Nature Mater.* **6** 183
[16] Geim A K, 2009 *Science* **324** 1530
[17] Balandin A A *et al*, 2008 *Nano Lett.* **8** 902
[18] Cai W *et al*, 2010 *Nano Lett.* **10** 1645
[19] Brenner D W *et al*, 2002 *J. Phys.: Condens. Matter* **14** 783
[20] Plimpton S, 1995 *J. Comput. Phys.* **117** 1
[21] Jund P and Jullien R, 1999 *Phys. Rev.* B **59** 13707
[22] Hu M, Keblinski P and Li B, 2008 *Appl. Phys. Lett.* **92** 211908
[23] Hu M, Keblinski P and Schelling P K, 2009 *Phys. Rev.* B **79** 104305
[24] Liang Z and Tsai H L, 2011 *Phys. Rev.* E **83** 041602
[25] Guo Z, Zhang D and Gong X G, 2009 *Appl. Phys. Lett.* **95** 163103
[26] Wei N, Xu L, Wang H Q and Zheng J C, 2011 *Nanotechnology* **22** 105705
[27] Ouyang T, Chen Y P, Yang K K and Zhong J X, 2009 *Europhys. Lett.* **88** 28002
[28] Hu J, Schiffli S, Vallabhaneni A, Ruan X and Chen Y P, 2010 *Appl. Phys. Lett.* **97** 133107
[29] Balasubramanian G, Puri I K, Bohm M C and Leroy F, 2011 *Nanoscale* **3** 3714
[30] Li X, Cai W, Colombo L and Ruoff R S, 2009 *Nano Lett.* **9** 4268
[31] Cheh J and Zhao H, 2011 arXiv:1107.3696v2 [cond-mat.mtrl-sci]
[32] Iizuka T and Wadati M, 1992 *J. Phys. Soc. Japan* **61** 3077

J. Stat. Mech. (2011) P10031

[33] Nesterenko V F, Daraio C, Herbold E B and Jin S, 2005 *Phys. Rev. Lett.* **95** 158702
[34] Vergara L, 2005 *Phys. Rev. Lett.* **95** 108002
[35] Wen Z and Zhao H, 2005 *Chin. Phys. Lett.* **22** 1340
[36] Zhao H, Wen Z, Zhang Y and Zheng D, 2005 *Phys. Rev. Lett.* **94** 025507
[37] Pereira E, 2011 *Phys. Rev.* E **83** 031106
[38] Astakhova T Y, Gurin O D, Menon M and Vinogradov G A, 2001 *Phys. Rev.* B **64** 035418
[39] Astakhova T Y, Menon M and Vinogradov G A, 2004 *Phys. Rev.* B **70** 125409

J. Stat. Mech. (2011) P10031